Letter

Puzzles in charmed baryon semileptonic decays with $SU(3)_F$ flavor symmetry and lattice inputs

Chao-Qiang Geng,[1] Chia-Wei Liu,[1] and Sheng-Lin Liu[1,2,3,*]

[1]*School of Fundamental Physics and Mathematical Sciences, Hangzhou Institute for Advanced Study, UCAS, Hangzhou 310024, China*

[2]*Institute of Theoretical Physics, UCAS, Beijing 100190, China*

[3]*University of Chinese Academy of Sciences, 100190 Beijing, China*

(Received 17 March 2026; accepted 28 May 2026; published 6 July 2026)

Recent measurements of charmed-baryon semileptonic decays signal large tensions between experiment and theory, including $SU(3)_F$ analyses and lattice-quantum chromodynamics simulations. Possible sources of the discrepancy include the experimental normalization mode $\Xi_c^0 \to \Xi^-\pi^+$. Using lattice-quantum chromodynamics inputs in an $SU(3)_F$ analysis including first-order symmetry breaking, we predict $\mathcal{B}(\Xi_c^+ \to \Sigma^0\ell^+\nu_\ell)/\mathcal{B}(\Xi_c^+ \to \Xi^0\ell^+\nu_\ell) = (2.6\pm0.3)\%$, and $\mathcal{B}(\Xi_c^+ \to \Lambda\ell^+\nu_\ell)/\mathcal{B}(\Xi_c^+ \to \Xi^0\ell^+\nu_\ell) = (1.1\pm0.1)\%$, with $\ell^+ = (e^+, \mu^+)$. These ratios provide normalization-independent tests and may help clarify the origin of the present tension.

DOI: 10.1103/h61y-61xw

Introduction. Significant discrepancies in $\mathcal{B}(\Xi_c^0 \to \Xi^- e^+\nu_e)$ have been found between the experimental data and theoretical studies, including lattice-quantum chromodynamics (LQCD). The relative branching fraction with respect to $\Xi_c^0 \to \Xi^-\pi^+$ was measured to be 0.730 ± 0.044 [1] and 0.825 ± 0.124 [2,3] at Belle and ALICE, respectively. Using the reference channel $\mathcal{B}(\Xi_c^0 \to \Xi^-\pi^+) = (1.43 \pm 0.27)\%$ [4], the corresponding absolute branching fractions are $(1.04 \pm 0.21)\%$ and $(1.18 \pm 0.28)\%$. In contrast, LQCD predicts $(2.48 \pm 0.86)\%$ [5] and $(3.58 \pm 0.12)\%$ [6]. On the other hand, $SU(3)_F$-based analyses predict that the absolute branching fraction should be around 4%, using $\Lambda_c^+ \to \Lambda e^+\nu_e$ measured at BESIII as input [7]. The $SU(3)_F$ prediction is in strong tension with the data, but in reasonably good agreement with the LQCD results. The experimental data indicate that the $SU(3)_F$ breaking exceeds 50%, and a theoretical understanding of this issue has remained elusive for more than half a decade.

Since both Belle and ALICE collaborations have reported convergent results, one naturally suspects that the discrepancy arises from an underestimation of the normalization channel $\mathcal{B}(\Xi_c^0 \to \Xi^-\pi^+)$ [8,9]. A determination of this branching fraction is crucial, as it is so far the only absolute branching fraction that has been measured for Ξ_c^0, and its uncertainty propagates into other measurements. Recently, a similar underestimation of the experimental branching fraction $\mathcal{B}(\Xi_c^+ \to \Xi^-\pi^+\pi^+)$ has also been conjectured [10,11]. In particular, the $SU(3)_F$ framework incorporating the Körner-Pati-Woo theorem suggests that this channel may be underestimated by a factor of two [8,9], with a discrepancy of about 4σ from the experimental result, although a fully satisfactory explanation remains under debate [12–14].

In this work, we parameterize the form factors of singly charmed baryon decays using $SU(3)_F$ flavor symmetry in the Bourrely-Caprini-Lellouch (BCL) z-expansion, including the first-order symmetry-breaking effects for the first time. The corresponding parameters are then determined from the LQCD results for these decays. The approximate symmetry among the light quarks provides a model-independent framework that has been widely applied to heavy-hadron decays [7–11,15–42]. We further propose golden channels that can help clarify the discrepancies observed experimentally.

This paper is organized as follows. In Sec. II, we present the formalism of the $SU(3)_F$ flavor-symmetry approach including first-order breaking. In Sec. III, we provide numerical results for the form factors, branching fractions, and angular observables of each channel, followed by discussions. Our conclusions are given in Sec. IV.

Formalism. The transitions of $\mathbf{B}_c \to \mathbf{B}\ell^+\nu_\ell$ induced by a current are best described by form factors, where $\ell^+ = (e^+, \mu^+)$ denotes the antileptons, and $\mathbf{B}_c$ and $\mathbf{B}$ stand for the charmed baryon and the octet baryon, respectively. In this work, we adopt the standard helicity form factors

*Contact author: liushenglin22@mails.ucas.ac.cn

and parameterize their q^2 dependence with the BCL z-expansion [43], defined by

$$f(q^2) = \frac{1}{1-q^2/(m_{\text{pole}}^f)^2}\sum_{n=0}^{n_{\max}} a_n^f [z_f(q^2)]^n,$$
$$z_f(q^2) = \frac{\sqrt{t_+^f - q^2} - \sqrt{t_+^f - t_0}}{\sqrt{t_+^f - q^2} + \sqrt{t_+^f - t_0}}.$$
$$f = f_+, f_\perp, f_0, g_+, g_\perp, g_0, \tag{1}$$

with $q = p_{\mathbf{B}_c} - p_{\mathbf{B}}$ and $t_0 = (m_{\mathbf{B}_c} - m_{\mathbf{B}})^2$. For $f = f_+, f_\perp, f_0$, the branch point $t_+^f = (m_D + m_{\pi(K)})^2$ is taken as the threshold of the $D\pi(K)$ two-particle states for the $c \to d(s)$ transitions, respectively. For $f = g_+, g_\perp, g_0$, the corresponding branch point is set by the $D^*\pi$ or D^*K thresholds, $t_+^f = (m_{D^*} + m_{\pi(K)})^2$. To satisfy the end point relations of $f_0(0) = f_+(0)$ and $g_0(0) = g_+(0)$, we choose

$$a_2^{f_0} = \frac{a_0^{f_+} - a_0^{f_0}}{z_{f_0}(0)^2} + \frac{a_1^{f_+} - a_1^{f_0}}{z_{f_0}(0)} + a_2^{f_+} + (a_3^{f_+} - a_3^{f_0}) z_{f_0}(0),$$
$$a_2^{g_0} = \frac{a_0^{g_+} - a_0^{g_0}}{z_{g_0}(0)^2} + \frac{a_1^{g_+} - a_1^{g_0}}{z_{g_0}(0)} + a_2^{g_+} + (a_3^{g_+} - a_3^{g_0}) z_{g_0}(0), \tag{2}$$

which were first used in Ref. [6].

The $SU(3)_F$ flavor-symmetry framework treats the light quarks u, d, and s on an equal footing, thereby classifying hadrons into multiplets corresponding to irreducible representations of $SU(3)_F$. The baryons are embedded in the $SU(3)_F$ representations

$$\mathbf{B}_c = (\Xi_c^0, -\Xi_c^+, \Lambda_c^+),$$
$$\mathbf{B} = \begin{pmatrix} \frac{1}{\sqrt{6}}\Lambda + \frac{1}{\sqrt{2}}\Sigma^0 & \Sigma^+ & p \\ \Sigma^- & \frac{1}{\sqrt{6}}\Lambda - \frac{1}{\sqrt{2}}\Sigma^0 & n \\ \Xi^- & \Xi^0 & -\sqrt{\frac{2}{3}}\Lambda \end{pmatrix}. \tag{3}$$

The coefficients a_n^f are $SU(3)_F$ singlets and, according to the generalized Wigner-Eckart theorem, can be parametrized as [44]

$$a_n^f = C_n^f (\mathbf{B}^\dagger)^\alpha_\beta \mathcal{J}^\beta (\mathbf{B}_c)_\alpha + V_n^f (\mathbf{B}^\dagger)^\alpha_\gamma \mathcal{J}^\beta \mathcal{S}^\gamma_\beta (\mathbf{B}_c)_\alpha$$
$$+ W_n^f (\mathbf{B}^\dagger)^\gamma_\beta \mathcal{J}^\beta \mathcal{S}^\alpha_\gamma (\mathbf{B}_c)_\alpha. \tag{4}$$

Here, $\mathcal{J}$ transforms in the same $SU(3)_F$ representation as q in $c \to q$ transitions. The first-order $SU(3)_F$-breaking effects are captured by the insertions of $\mathcal{S} = \text{diag}(1,1,-2)/\sqrt{6}$ with the parameters V_n^f and W_n^f, which are of order m_s/Λ_{QCD}. In the $SU(3)_F$ limit, $V_n^f = W_n^f = 0$. In the above equations, the relevant components of $\mathbf{B}_c$ and $\mathbf{B}$ are selected by flavor indices. For instance, for the $c \to s$ transition of $\Lambda_c^+ \to \Lambda$, one takes

$$\mathbf{B}_c = \mathcal{J}^\dagger = (0,0,1), \qquad \mathbf{B} = \text{diag}\left(\sqrt{\frac{1}{6}}, \sqrt{\frac{1}{6}}, -\sqrt{\frac{2}{3}}\right), \tag{5}$$

resulting in

$$a_n^f(\Lambda_c \to \Lambda) = -\sqrt{\frac{2}{3}} C_n^f + \frac{2}{3} V_n^f + \frac{2}{3} W_n^f. \tag{6}$$

The same flavor structure applies to the other form factors as well.

Numerical results. We take the LQCD results [6,46,47] as input, including the form factors for $\Lambda_c^+ \to \Lambda$, $\Lambda_c^+ \to n$, and $\Xi_c \to \Xi$. From Eq. (4) we solve C_n^f, V_n^f, and W_n^f by

$$\begin{pmatrix} C_n^f \\ V_n^f \\ W_n^f \end{pmatrix} = \begin{pmatrix} \frac{1}{\sqrt{6}} & \frac{2}{3} & \frac{2}{3} \\ 1 & \sqrt{\frac{2}{3}} & 0 \\ 1 & 0 & \sqrt{\frac{2}{3}} \end{pmatrix} \begin{pmatrix} a_n^f(\Lambda_c \to \Lambda) \\ a_n^f(\Lambda_c \to n) \\ a_n^f(\Xi_c \to \Xi) \end{pmatrix}. \tag{7}$$

A slightly different BCL z-expansion was adopted in Refs. [46,47]. The corresponding expansion variable is similar to $z_f(q^2)$ defined in Eq. (1), except that $t_+^f = (m_D + m_{\pi(K)})^2$ for $f = g_0, g_+, g_\perp$. We denote the variable therein by $\tilde{z}_f(q^2)$ and match it to $z_f(q^2)$ used in this work, as described in the Appendix. The numerical results are presented in Table I. The resulting form factors for $\Xi_c \to \Xi$ are essentially identical to those from LQCD [6], while we have checked that those for $\Lambda_c^+ \to \Lambda, n$ also reproduce the LQCD results up to $\mathcal{O}(10^{-3})$ [46,47]. Since $|z_f| < 0.16$ over the physical region, the form factors are dominated by the terms with $n = 0$. From the table, one can see that the typical sizes of V_0^f/C_0^f and W_0^f/C_0^f are around 10% to 20%, as expected in the usual $SU(3)_F$ framework. Errors from truncating the $SU(3)_F$ breaking are therefore expected to be of order 10^{-2}.

The genuinely new predictions are those for $\Xi_c^+ \to \Lambda$ and $\Xi_c^+ \to \Sigma^0$ given in Table II, with the coefficients

$$\begin{pmatrix} a_n^f(\Xi_c^+ \to \Lambda) \\ a_n^f(\Xi_c^+ \to \Sigma^0) \end{pmatrix} = \begin{pmatrix} -\frac{1}{\sqrt{6}} & -\frac{1}{6} & -\frac{1}{6} \\ \frac{1}{\sqrt{2}} & \frac{1}{2\sqrt{3}} & \frac{1}{2\sqrt{3}} \end{pmatrix} \begin{pmatrix} C_n^f \\ V_n^f \\ W_n^f \end{pmatrix}. \tag{8}$$

The isospin symmetry implies that a_n^f of $\Xi_c^0 \to \Sigma^-$ is $\sqrt{2}$ times larger than those of $\Xi_c^+ \to \Sigma^0$ and for simplicity we list only the form factors for the latter channel. Since $|z_f(q^2)| < 0.16$ for all form factors f, the contributions from higher-order terms are strongly suppressed.

TABLE I. Numerical results for the BCL z expansion with $SU(3)_F$ symmetry including first-order breaking. The uncertainties are taken from the LQCD calculations [6,46,47].

(f,n)	C_n^f	V_n^f	W_n^f
$(f_\perp,0)$	1.528(71)	−0.202(103)	0.155(82)
$(f_\perp,1)$	−4.093(945)	1.764(1.564)	−2.502(1.436)
$(f_\perp,2)$	4.5(8.6)	−8(14)	3(13)
$(f_\perp,3)$	1(30)	7(38)	−4(39)
$(f_+,0)$	0.849(39)	−0.137(55)	−0.009(40)
$(f_+,1)$	−3.310(679)	0.796(913)	−1.280(714)
$(f_+,2)$	11.7(6.8)	−2.3(8.9)	6.6(7.4)
$(f_+,3)$	−6(30)	9(38)	−16(38)
$(f_0,0)$	0.838(40)	−0.090(54)	−0.023(36)
$(f_0,1)$	−3.206(694)	−0.206(924)	−1.066(679)
$(f_0,3)$	3(30)	8(38)	−4(38)
$(g_\perp,0)$	0.689(26)	−0.115(36)	−0.046(26)
$(g_\perp,1)$	−2.134(500)	1.077(722)	−0.690(609)
$(g_\perp,2)$	8.8(6.2)	−2.9(8.7)	0.7(7.7)
$(g_\perp,3)$	−8(28)	−17(36)	19(38)
$(g_+,0)$	0.689(26)	−0.115(36)	−0.046(26)
$(g_+,1)$	−2.161(434)	1.460(571)	−0.251(413)
$(g_+,2)$	5.8(5.4)	−11.8(6.9)	−6.6(5.6)
$(g_+,3)$	−3(28)	−15(35)	−3(37)
$(g_0,0)$	0.737(40)	−0.140(56)	−0.037(39)
$(g_0,1)$	−2.893(611)	2.277(821)	−0.959(615)
$(g_0,3)$	−2(29)	2(37)	8(38)

Consequently, the uncertainties of the form factors are dominated by those of the coefficients $a_n^f(C_n^f, V_n^f, W_n^f)$ with $n=0$ and $n=1$. The form factors are explicitly depicted in Fig. 1.

In addition to the branching fractions, experiments have measured the up-down asymmetries defined by

TABLE II. The numerical results of z-expansion parameters for $\Xi_c^+ \to \Lambda$ and $\Xi_c^+ \to \Sigma^0$. The parameters of $a_2^{f_0}$ and $a_2^{g_0}$ can be obtained by Eq. (2).

	$\Xi_c^+ \to \Lambda$		$\Xi_c^+ \to \Sigma^0$	
(i,n)	$a_n^{f_i}$	$a_n^{g_i}$	$a_n^{f_i}$	$a_n^{g_i}$
$(\perp,0)$	−0.62(5)	−0.25(2)	1.07(9)	0.44(3)
$(\perp,1)$	1.79(82)	0.81(39)	−3.11(1.42)	−1.40(67)
$(\perp,2)$	−1(7)	−3.2(4.8)	2(13)	5.6(8.3)
$(\perp,3)$	−1(23)	3(22)	1(39)	−5(38)
$(+,0)$	−0.32(3)	−0.25(2)	0.56(5)	0.44(3)
$(+,1)$	1.43(49)	0.68(31)	−2.48(85)	−1.18(53)
$(+,2)$	−5(5)	0.7(3.8)	9.5(8.6)	−1.2(6.7)
$(+,3)$	4(22)	4(21)	−6(39)	−8(37)
(0, 0)	−0.32(3)	−0.27(3)	0.56(5)	0.47(5)
(0, 1)	1.52(49)	0.96(44)	−2.64(86)	−1.67(76)
(0, 3)	−2(22)	−1(22)	3(39)	2(38)

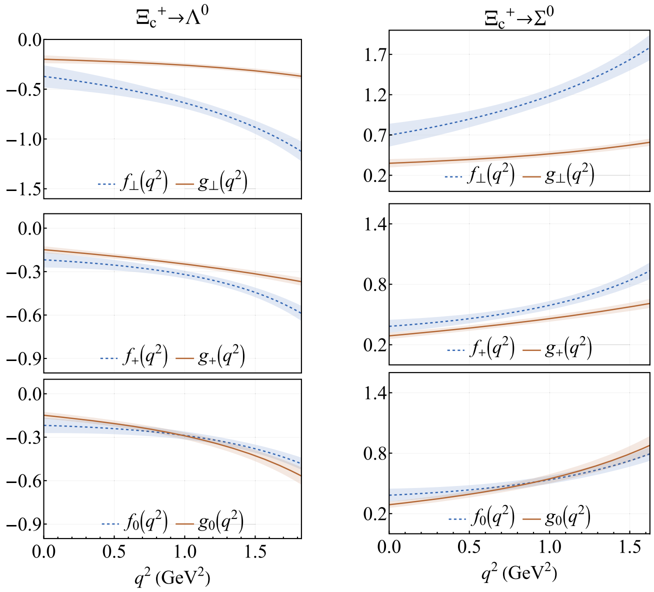

FIG. 1. The numerical results of form factors $f_\perp, f_+, f_0, g_\perp, g_+$ and g_0 from the $SU(3)_F$ approach of $\Xi_c^+ \to \Lambda$ and $\Xi_c^+ \to \Sigma^0$.

$$\alpha = \frac{\Gamma_+ - \Gamma_-}{\Gamma_+ + \Gamma_-}, \tag{9}$$

where $\Gamma_\pm$ denote the partial rates into final-baryon helicity $\lambda_{\mathbf{B}} = \pm 1/2$. For $\Lambda_c^+ \to \Lambda e^+ \nu_e$, it can be measured by the sequential decay of $\Lambda \to p\pi^-$ [48–52]. Utilizing the CKM matrix elements $V_{cd} = 0.225 \pm 0.004$ and $V_{cs} = 0.975 \pm 0.006$ from the latest CKMfitter results [53], together with the lifetimes of singly charmed baryons reported by the PDG [4], we evaluate the branching fractions and up-down asymmetries for channels $\Xi_c^+ \to \Lambda$ and $\Xi_c \to \Sigma$ in Table III, where the results are genuine new predictions established in this work.

As discussed in the Introduction, the puzzle may be traced back to the normalization channel. To test the $SU(3)_F$ breaking in a normalization-independent way, we propose to measure the relative branching fractions to $\Xi_c \to \Xi \ell^+ \nu_\ell$. In particular, we predict the ratios

TABLE III. Numerical results for branching fractions and up-down asymmetries in the $SU(3)_F$ approach for the channels $\Xi_c^+ \to \Lambda$ and $\Xi_c \to \Sigma$, in units of percentage.

Channels	$\mathcal{B}(SU(3)_F)(\%)$	$\alpha(SU(3)_F)(\%)$
$\Xi_c^+ \to \Sigma^0 e^+ \nu_e$	0.282(30)	−89.9(9.3)
$\Xi_c^+ \to \Sigma^0 \mu^+ \nu_\mu$	0.275(29)	−89.7(9.2)
$\Xi_c^+ \to \Lambda e^+ \nu_e$	0.117(14)	−90.8(10.2)
$\Xi_c^+ \to \Lambda \mu^+ \nu_\mu$	0.115(13)	−90.7(10.1)
$\Xi_c^0 \to \Sigma^- e^+ \nu_e$	0.186(20)	−89.8(9.3)
$\Xi_c^0 \to \Sigma^- \mu^+ \nu_\mu$	0.182(19)	−89.7(9.2)

TABLE IV. Values of R_{Σ^0} and R_Λ for the exact $SU(3)_F$ symmetry scheme, for our $SU(3)_F$ symmetry analysis matched to LQCD inputs from Eq. (10), and for the first-order $SU(3)_F$-breaking analysis of Ref. [7], where the input parameters were determined from experimental data.

Values	Exact $SU(3)_F$	$SU(3)_F$ + LQCD	$SU(3)_F$+ Exp. [7]
$R_{\Sigma^0}(\%)$	2.6	2.6 ± 0.3	12.8 ± 2.7
$R_\Lambda(\%)$	0.9	1.1 ± 0.1	1.7 ± 0.5

$$R_{\Sigma^0} \equiv \frac{\mathcal{B}(\Xi_c^+ \to \Sigma^0 \ell^+ \nu_\ell)}{\mathcal{B}(\Xi_c^+ \to \Xi^0 \ell^+ \nu_\ell)} = (2.6 \pm 0.3)\%,$$
$$R_\Lambda \equiv \frac{\mathcal{B}(\Xi_c^+ \to \Lambda \ell^+ \nu_\ell)}{\mathcal{B}(\Xi_c^+ \to \Xi^0 \ell^+ \nu_\ell)} = (1.1 \pm 0.1)\%,$$
$$R_{\Sigma^-} \equiv \frac{\mathcal{B}(\Xi_c^0 \to \Sigma^- \ell^+ \nu_\ell)}{\mathcal{B}(\Xi_c^0 \to \Xi^- \ell^+ \nu_\ell)} = 2R_{\Sigma^0}, \tag{10}$$

which are protected up to second order in $SU(3)_F$ breaking, with expected precision at the percent level. These ratios have the advantage of avoiding the normalization ambiguity associated with $\mathcal{B}(\Xi_c^0 \to \Xi^- \pi^+)$.

In Table IV, we compare the values of $R_\mathbf{B}$ obtained in the exact $SU(3)_F$ limit, in our $SU(3)_F$ + LQCD analysis, and in the first-order $SU(3)_F$-breaking analysis using the experimental inputs $\mathcal{B}(\Lambda_c^+ \to \Lambda \ell^+ \nu_\ell)$ and $\mathcal{B}(\Xi_c \to \Xi \ell^+ \nu_\ell)$ [7]. Our results are very close to the exact-$SU(3)_F$ predictions, indicating that the relevant first-order $SU(3)_F$-breaking effects are small according to LQCD. By contrast, the data-driven first-order analysis [7] gives a much larger value of R_{Σ^0}, about five times larger than both the exact-$SU(3)_F$ and $SU(3)_F$ + LQCD predictions. If future measurements favor the exact-$SU(3)_F$ and $SU(3)_F$ + LQCD predictions, this would point to the normalization input used in Ref. [7], $\mathcal{B}(\Xi_c^0 \to \Xi^- \pi^+) = (1.80 \pm 0.50 \pm 0.14)\%$ as a likely source of the tension. In this case, since the semileptonic ratios would be consistent with both $SU(3)_F$ symmetry and LQCD, the discrepancy would more naturally be attributed to the experimental normalization channel $\Xi_c^0 \to \Xi^- \pi^+$ than to large unknown hadronic effects in the semileptonic form factors. Conversely, if the measurements favor the data-driven first-order result, this would suggest that additional hadronic effects beyond those captured by the LQCD-matched $SU(3)_F$ analysis may be required.

We now discuss the experimental testability. The numbers of observed events are expected to be

$$\frac{N(\Xi_c \to \mathbf{B} e^+ \nu_e)}{N(\Xi_c \to \Xi e^+ \nu_e)} = R_\mathbf{B} \frac{\epsilon_\mathbf{B}}{\epsilon_\Xi}, \tag{11}$$

where $\epsilon_\mathbf{B}$ is the reconstruction efficiency for the final-state baryon $\mathbf{B}$. The number of produced Ξ_c^+ baryons at Belle and Belle II is not directly known. For an order-of-magnitude estimate, we assume comparable production rates for Ξ_c^+ and Ξ_c^0, as suggested by approximate isospin symmetry in charm fragmentation. This approximation is based on the assumption that the $c\bar{c}$ pair is produced via γ^*, thereby minimizing the number of hard gluons, along with the use of isospin symmetry. We take the efficiencies to be $(\epsilon_{\Xi^0}, \epsilon_{\Sigma^0}, \epsilon_\Lambda, \epsilon_{\Xi^-}) = (1.5\%, 7\%, 20\%, 20\%)$ [54–56]. In 2021, $(16.01 \pm 0.44) \times 10^3$ events were observed for $\Xi_c^0 \to \Xi^- e^+ \nu_e$ with an integrated luminosity of $711 + 89.5 = 800.5\ \mathrm{fb}^{-1}$ at $\sqrt{s} = 10.58$ and 10.52 GeV at Belle [1]. At present, the combined integrated luminosity of Belle and Belle II has reached $1.8\ \mathrm{ab}^{-1}$ [57,58]. Based on the Belle measurements and naively assuming the same reconstruction efficiencies at Belle and Belle II, we estimate the expected statistical precisions to be $(\delta R_{\Sigma^0}, \delta R_\Lambda) \approx (0.40\%, 0.13\%)$. This estimate should be regarded as conservative, since the improved performance of the Belle II detector is expected to lead to higher reconstruction efficiencies than those at Belle [59–61]. With the future Belle II dataset, whose integrated luminosity is expected to reach $50\ \mathrm{ab}^{-1}$ [62], the statistical precision would improve by at least about a factor of six.

The simulations of the experiments for these channels are presented in Fig. 2, and the label "Belle + Belle II"

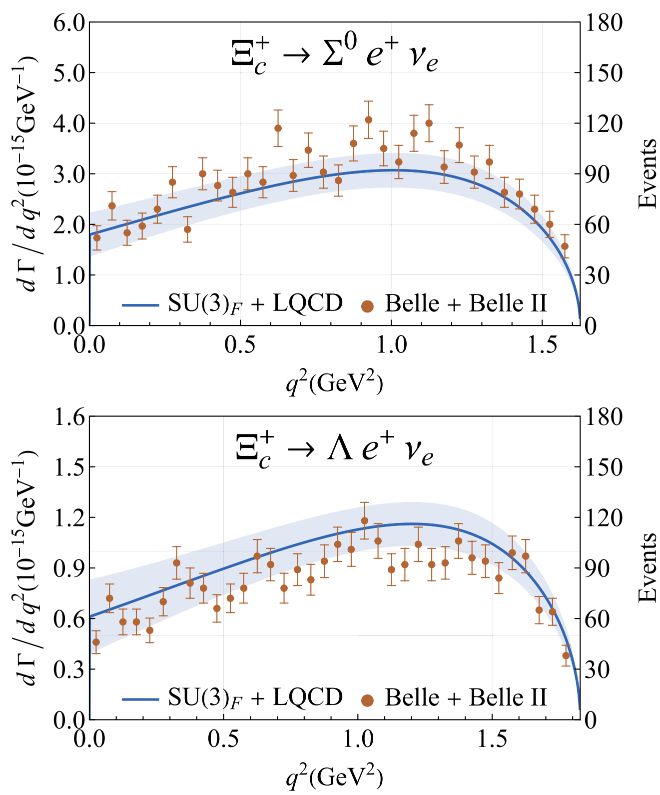

FIG. 2. Differential decay rates and estimated event yields for $\Xi_c^+ \to \Sigma^0 e^+ \nu_e$ and $\Xi_c^+ \to \Lambda e^+ \nu_e$. The q^2 dependence of the differential decay rates is shown on the left Y-axis, while the event yields estimated by scaling to $\mathcal{L}_{\mathrm{int}} = 1.8\ \mathrm{ab}^{-1}$ are shown on the right Y-axis.

denotes an order-of-magnitude scaling to a combined integrated luminosity $\mathcal{L}_{\rm int} = 1.8\ \mathrm{ab}^{-1}$. Throughout the simulations, we assume that the detection efficiencies are independent of q^2, while the $\sqrt{q^2}$-bin widths are fixed at 50 MeV. From the figure, one sees that the expected signal yields are sizable across a wide range of $\sqrt{q^2}$, suggesting that the differential spectra are experimentally measurable with sufficient statistics.

Since the dominant decay $\Sigma^- \to n\pi^-$ contains a neutron in the final state, this channel is difficult to reconstruct at Belle and Belle II. It could, however, be reconstructed at BESIII and STCF, with an estimated efficiency $\epsilon_{\Sigma^-} = 14.3\%$ [63]. So far, the production numbers of Ξ_c are not known. Assuming that the near-threshold $\Xi_c\bar{\Xi}_c$ production rate is about $0.1 \sim 0.3$ of that for $e^+e^- \to \Lambda_c^+\bar{\Lambda}_c^-$, one is led to a benchmark cross section $\sigma(e^+e^- \to \Xi_c\bar{\Xi}_c) \sim 10$–$30$ pb [64,65]. With the approved BEPCII upgrade, the maximum center-of-mass energy will be extended to 5.6 GeV, while the peak luminosity at high energies is expected to increase by about a factor of three [66]. This will enable direct studies of $\Xi_c\bar{\Xi}_c$ production; for a benchmark cross section $\sigma(e^+e^- \to \Xi_c\bar{\Xi}_c) \sim 10$–$30$ pb, one expects roughly $(1-3)\times 10^5$ produced pairs per year at peak luminosity at BEPCII-U, while the corresponding yield at the STCF would be about $(1-3)\times 10^7$ pairs per year [67].

Conclusions. We have developed an $SU(3)_F$ analysis of singly charmed baryon semileptonic decays by matching the available lattice-QCD form factors onto the BCL z-expansion, including first-order symmetry-breaking effects. The resulting framework consistently reproduces the known lattice inputs and yields symmetry-breaking corrections of the expected size.

With these inputs, we have predicted the form factors and decay observables for $\Xi_c^+ \to \Lambda\ell^+\nu_\ell$ and $\Xi_c \to \Sigma\ell^+\nu_\ell$. In particular, we identified the ratios $(R_{\Sigma^-}, R_{\Sigma^0}, R_\Lambda) = (5.2 \pm 0.6, 2.6 \pm 0.3, 1.1 \pm 0.1)\%$. These ratios are free from the normalization ambiguity associated with $\mathcal{B}(\Xi_c^0 \to \Xi^-\pi^+)$ and $\mathcal{B}(\Xi_c^+ \to \Xi^-\pi^+\pi^+)$. They therefore provide normalization-independent probes of the first-order $SU(3)_F$ breaking.

We have also shown that the corresponding signal yields should be experimentally measurable within the Belle + Belle II luminosity estimate, subject to detector-specific efficiencies and systematic uncertainties. The expected statistical precisions are $(\delta R_{\Sigma^0}, \delta R_\Lambda) \simeq (4.0, 1.3)\times 10^{-3}$. Precise determinations of these ratios would provide normalization-independent tests of $SU(3)_F$ breaking and help clarify whether the current puzzle originates from an underestimation of the nonleptonic $\Xi_c^0 \to \Xi^-\pi^+$ decay or from unknown hadronic effects.

Acknowledgments. We would like to express our sincere appreciation to Long-Ke Li for the valuable discussions. This work is supported in part by the National Natural Science Foundation of China (NSFC) under Grants No. 12547104 and No. 12575096.

Data availability. The data that support the findings of this article are openly available [6,46,47].

Appendix: Matching z-expansion conventions. Expanding $\tilde{z}_f$ in powers of z_f, we obtain formally

$$\tilde{z}_f = d_0 + d_1 z_f + d_2 z_f^2 + d_3 z_f^3 + \mathcal{O}(z_f^4), \tag{A1}$$

where d_n is defined by

$$d_n^f = \frac{1}{n!}\frac{d^n\tilde{z}_f}{dz_f^n}\bigg|_{z_f=0} = \frac{1}{n!}\left(\frac{dq^2}{dz_f}\frac{d}{dq^2}\right)^n \tilde{z}_f(q^2)\bigg|_{z_f=0}. \tag{A2}$$

The explicit form is too lengthy to be informative and can be calculated by a modern computer program.

We denote the BCL coefficients in the expansion in $\tilde{z}_f$ by $\tilde{a}_n^f$, and impose the matching condition

$$\sum_n a_n^f z_f^n = \sum_n \tilde{a}_n^f \tilde{z}_f^n. \tag{A3}$$

This leads to the relations

$$\begin{aligned}
a_0^f &= \tilde{a}_0^f + \tilde{a}_1^f d_0^f + \tilde{a}_2^f (d_0^f)^2 + \tilde{a}_3^f (d_0^f)^3,\\
a_1^f &= \tilde{a}_1^f d_1^f + 2\tilde{a}_2^f d_0^f d_1^f + 3\tilde{a}_3^f (d_0^f)^2 d_1^f,\\
a_2^f &= \tilde{a}_1^f d_2^f + \tilde{a}_2^f[(d_1^f)^2 + 2d_0^f d_2^f]\\
&\quad + \tilde{a}_3^f[3d_0^f(d_1^f)^2 + 3(d_0^f)^2 d_2^f],\\
a_3^f &= \tilde{a}_1^f d_3^f + 2\tilde{a}_2^f(d_0^f d_3^f + d_1^f d_2^f)\\
&\quad + \tilde{a}_3^f[(d_1^f)^3 + 6d_0^f d_1^f d_2^f + 3(d_0^f)^2 d_3^f],
\end{aligned} \tag{A4}$$

up to the precision of $|z_f^4(q^2)| < 10^{-3}$. We note that $\tilde{a}_n^f$ is denoted simply by a_n^f in Refs. [46,47]. The above relations therefore allow us to match their parametrization to the one in this work.

[1] Y. B. Li *et al.* (Belle Collaboration), Phys. Rev. Lett. **127**, 121803 (2021).
[2] S. Acharya *et al.* (ALICE Collaboration), Phys. Rev. Lett. **127**, 272001 (2021); **134**, 179902(E) (2025).
[3] I. J. Abualrob *et al.* (ALICE Collaboration), J. High Energy Phys. 12 (2025) 038.
[4] S. Navas *et al.* (Particle Data Group), Phys. Rev. D **110**, 030001 (2024).
[5] Q. A. Zhang, J. Hua, F. Huang, R. Li, Y. Li, C. Lü, C. D. Lu, P. Sun, W. Sun, W. Wang, and Y. Yang, Chin. Phys. C **46**, 011002 (2022).
[6] C. Farrell and S. Meinel, Phys. Rev. D **111**, 114521 (2025).
[7] X. G. He, F. Huang, W. Wang, and Z. P. Xing, Phys. Lett. B **823**, 136765 (2021).
[8] C. Q. Geng, X. G. He, X. N. Jin, C. W. Liu, and C. Yang, Phys. Rev. D **109**, L071302 (2024).
[9] H. Y. Cheng, F. Xu, and H. Zhong, Phys. Rev. D **111**, 034011 (2025).
[10] C. Q. Geng, C. W. Liu, and S. L. Liu, Phys. Rev. D **109**, 093002 (2024).
[11] C. Yang, X. G. He, and C. W. Liu, J. High Energy Phys. 09 (2025) 193.
[12] T. M. Aliev, S. Bilmis, and M. Savci, Phys. Rev. D **104**, 054030 (2021).
[13] D. Wang, arXiv:2507.06914.
[14] T. M. Aliev, S. Bilmis, and M. Savci, Phys. Rev. D **113**, 014008 (2026).
[15] M. J. Savage and R. P. Springer, Phys. Rev. D **42**, 1527 (1990).
[16] M. J. Savage, Phys. Lett. B **257**, 414 (1991).
[17] D. Pirtskhalava and P. Uttayarat, Phys. Lett. B **712**, 81 (2012).
[18] Y. Grossman and D. J. Robinson, J. High Energy Phys. 04 (2013) 067.
[19] C. D. Lü, W. Wang, and F. S. Yu, Phys. Rev. D **93**, 056008 (2016).
[20] C. Q. Geng, Y. K. Hsiao, Y. H. Lin, and L. L. Liu, Phys. Lett. B **776**, 265 (2018).
[21] C. Q. Geng, Y. K. Hsiao, C. W. Liu, and T. H. Tsai, J. High Energy Phys. 11 (2017) 147.
[22] D. Wang, P. F. Guo, W. H. Long, and F. S. Yu, J. High Energy Phys. 03 (2018) 066.
[23] C. Q. Geng, Y. K. Hsiao, C. W. Liu, and T. H. Tsai, Phys. Rev. D **97**, 073006 (2018).
[24] C. Q. Geng, Y. K. Hsiao, C. W. Liu, and T. H. Tsai, Eur. Phys. J. C **78**, 593 (2018).
[25] C. Q. Geng, C. W. Liu, and T. H. Tsai, Phys. Lett. B **790**, 225 (2019).
[26] C. Q. Geng, Y. K. Hsiao, C. W. Liu, and T. H. Tsai, Phys. Rev. D **99**, 073003 (2019).
[27] J. Y. Cen, C. Q. Geng, C. W. Liu, and T. H. Tsai, Eur. Phys. J. C **79**, 946 (2019).
[28] Y. K. Hsiao, Y. Yao, and H. J. Zhao, Phys. Lett. B **792**, 35 (2019).
[29] C. Q. Geng, C. W. Liu, T. H. Tsai, and Y. Yu, Phys. Rev. D **99**, 114022 (2019).
[30] C. Q. Geng, C. W. Liu, T. H. Tsai, and S. W. Yeh, Phys. Lett. B **792**, 214 (2019).
[31] C. P. Jia, D. Wang, and F. S. Yu, Nucl. Phys. **B956**, 115048 (2020).
[32] C. Q. Geng, C. W. Liu, and T. H. Tsai, Phys. Lett. B **794**, 19 (2019).
[33] C. W. Liu, Phys. Rev. D **109**, 033004 (2024).
[34] Y. K. Hsiao, J. High Energy Phys. 11 (2023) 117.
[35] H. Zhong, F. Xu, and H. Y. Cheng, arXiv:2401.15926.
[36] H. Zhong, F. Xu, and H. Y. Cheng, Phys. Rev. D **109**, 114027 (2024).
[37] X. G. He and C. W. Liu, Sci. Bull. **70**, 2598 (2025).
[38] J. Sun, Z. P. Xing, and R. Zhu, Eur. Phys. J. C **85**, 262 (2025).
[39] Z. P. Xing, Y. J. Shi, J. Sun, and Y. Xing, Eur. Phys. J. C **84**, 1014 (2024).
[40] C. Q. Geng, C. W. Liu, and S. L. Liu, J. High Energy Phys. 07 (2025) 151.
[41] X. Wu, Q. Chen, Y. Xing, Z. P. Xing, and R. Zhu, Chin. Phys. C **49**, 123101 (2025).
[42] H. Y. Cheng, F. Xu, and H. Zhong, Phys. Rev. D **112**, 054022 (2025).
[43] C. Bourrely, I. Caprini, and L. Lellouch, Phys. Rev. D **79**, 013008 (2009); **82**, 099902(E) (2010).
[44] In general, there is an additional $SU(3)_F$ invariant: $a_n^f \ni U_n^f \mathrm{Tr}(\mathbf{B}^\dagger \mathcal{S})\mathcal{J}^\beta(\mathbf{B}_c)_\beta = \Lambda^\dagger(1115)\mathcal{J}^\beta(\mathbf{B}_c)_\beta$, which parametrizes the effects of mixing between $\Lambda(1115)$ and singlet Λ excitations, such as $\Lambda(1710)$ [45]. However, such mixing would shift the mass of $\Lambda(1115)$, and there is no evidence from the mass spectrum that this effect is required. We therefore set $U_n^f = 0$.
[45] E. Klempt, V. Burkert, U. Thoma, L. Tiator, and R. Workman (Baryon@PDG Group), Eur. Phys. J. A **56**, 261 (2020).
[46] S. Meinel, Phys. Rev. Lett. **118**, 082001 (2017).
[47] S. Meinel, Phys. Rev. D **97**, 034511 (2018).
[48] M. Ablikim *et al.* (BESIII Collaboration), Phys. Rev. D **100**, 072004 (2019).
[49] L. K. Li *et al.* (Belle Collaboration), Sci. Bull. **68**, 583 (2023).
[50] M. Ablikim *et al.* (BESIII Collaboration), J. High Energy Phys. 12 (2022) 033.
[51] M. Ablikim *et al.* (BESIII Collaboration), Phys. Rev. D **108**, L031105 (2023).
[52] R. Aaij *et al.* (LHCb Collaboration), Phys. Rev. Lett. **133**, 261804 (2024).
[53] J. Charles *et al.* (CKMfitter Group), Eur. Phys. J. C **41**, 1–131 (2005).
[54] I. Adachi *et al.* (Belle and Belle-II Collaborations), J. High Energy Phys. 10 (2024) 045.
[55] S. Jia *et al.* (Belle Collaboration), J. High Energy Phys. 06 (2021) 160.
[56] Y. Li *et al.* (Belle Collaboration), Phys. Rev. D **105**, L011102 (2022).
[57] J. Yelton *et al.* (Belle Collaboration), Phys. Rev. D **97**, 051102 (2018).
[58] Belle II Collaboration, https://www.belle2.org/info/luminosity_status/index_html#2026a.
[59] H. Aihara, A. Aloisio, D. P. Auguste, M. Aversano, M. Babeluk, S. Bahinipati, S. Banerjee, M. Barbero, J. Baudot, A. Beaubien *et al.*, arXiv:2406.19421.
[60] F. Bernlochner *et al.* (Belle-II Collaboration), arXiv:2503.24155.
[61] I. Adachi *et al.* (Belle-II Collaboration), Eur. Phys. J. C **85**, 1237 (2025).

[62] E. Kou *et al.* (Belle-II Collaboration), Prog. Theor. Exp. Phys. **2019**, 123C01 (2019); **2020**, 029201(E) (2020).
[63] M. Ablikim *et al.* (BESIII Collaboration), Phys. Rev. D **113**, 072014 (2026).
[64] M. Ablikim *et al.* (BESIII Collaboration), Phys. Rev. Lett. **131**, 191901 (2023).
[65] M. Ablikim *et al.* (BESIII Collaboration), Chin. Phys. C **46**, 113003 (2022).
[66] H. B. Li *et al.* (BESIII Collaboration), arXiv:2204.08943.
[67] M. Achasov, X. C. Ai, R. Aliberti, L. P. An, Q. An, X. Z. Bai, Y. Bai, O. Bakina, A. Barnyakov, and V. Blinov *et al.*, Front. Phys. (Beijing) **19**, 14701 (2024).